ORIGINAL PAPER

Aptamer-functionalized gold nanoparticles for mercury ion detection in a colorimetric assay based on color change time as signal readout

Bin Cai[1] · Tingyan Ren[1] · Xiaowei Yu[1] · Wendong Lv[2] · Yong Liang[3]

Abstract

A universal strategy for a rapid colorimetric method for Hg^{2+} in an aqueous solution is described. The specific binding of Hg^{2+} (thymine-Hg^{2+}-thymine) with thiolated DNA-functionalized gold nanoparticles (AuNPs) via Au–S bonds increases the spatial hindrance of the AuNP surface, resulting in a weakened catalytic ability of AuNPs to catalyze the reaction between p-nitrophenol and $NaBH_4$. Therefore, the color change time (CCT) of the solution from yellow to colorless becomes longer. Based on the kinetic curve of absorbance over time measured by a UV spectrometer, the level of Hg^{2+} in aqueous solutions can be easily quantified. A linear relationship between CCT and Hg^{2+} concentration was obtained in the 10–600-nM range with a detection limit of 0.20 nM, which is much lower than the limit value (10 nM) defined by the US Environmental Protection Agency for Hg^{2+} in drinking water. The excellent sensitivity comes from CCT as the signal output of the probe, rather than the absorbance or wavelength change used in traditional colorimetric probes as the signal output.

Keywords Visual observation · Spatial hindrance · Nanoprobe · Thymine-Hg^{2+}-thymine · Kinetic determination

Introduction

Heavy metal ions are the main source of water pollution and toxicity. Among them, the pollution of water-soluble Hg^{2+} is listed by the World Health Organization (WHO) as one of the 10 pollutants that pose a threat to public health [1, 2]. According to the standards of the United States Environmental Protection Agency (EPA), the maximum allowable limit for Hg^{2+} in drinking water is 10 nM [3–5]. Therefore, there is an urgent need for an efficient, highly sensitive, and selective method for monitoring Hg^{2+} in water solutions.

In recent years, various advances have been made for sensing Hg^{2+}, including fluorescence [6–8], electrochemistry [9–11], and colorimetric methods [12–15]. Fluorometry and electrochemical methods require qualified personnel and complex sample processing. Whereas colorimetric methods have received great attention due to the advantages such as easy operation, fast response, signal visibility (instrument-free), suitability for on-site, and high throughput analysis [16, 17]. Compared with other metal ions, Hg^{2+} ions have some significant characteristics as they can bind to nucleic acid aptamers rich in thymine (T), forming a very stable T-Hg T structure [18, 19].

It is widely known that noble metal nanoparticles (such as AuNPs and AgNPs) exhibit strong surface plasmon resonance (SPR) absorption from visible to near-infrared region; the aggregation of AuNPs induces electric dipole- interaction and coupling between adjacent particle plasmons, resulting in a color change to purple or blue, making them commonly used as colorimetric probes in the sensing field [20–22]. However, the large AuNP aggregates reduce the sensitivity of the assay, and the color changes of the aggregates are difficult to distinguish, which undoubtedly limits their practical application.

Herein, we propose a very simple and effective colorimetric method for quantifying Hg^{2+} concentration.

✉ Wendong Lv
  lwdwt@163.com

✉ Yong Liang
  liangy@scnu.edu.cn

[1] Ministry of Ecology and Environment, South China Institute of Environmental Science, Guangzhou 510655, China

[2] Institute of Resources Utilization and Rare Earth Development, Guangdong Academy of Sciences, Guangzhou 510650, China

[3] School of Chemistry, South China Normal University, Guangzhou 510631, China

As illustrated in Scheme 1, in this probe design, DNA strands with abundant T bases that are thiolated at the 5′ end are connected to the AuNP surface through Au–S bonds. In the absence of target Hg^{2+}, the yellow 4-nitrophenol easily approaches the catalytic surface of AuNPs and transforms into colorless 4-aminophenol. While in the presence of Hg^{2+}, the formation of T-Hg^{2+}-T complexes leads to the surface of AuNPs being covered, which in turn weakens the catalytic ability of the AuNPs and increases the color change time (CCT) of the solution from yellow 4-nitrophenol to colorless 4-aminophenol. Due to the repulsion generated by the negative charges carried by the AuNPs and DNA connected to AuNPs, AuNPs will not aggregate, thus avoiding errors caused by the AuNP aggregation. This can be well verified by the ultraviolet–visible spectroscopy (UV–vis) spectra, dynamic light scattering (DLS) size distribution, and transmission electron microscope (TEM) characterizations of AuNPs before and after the addition of Hg^{2+}, as shown in Figure S1-Figure S3, throughout the entire experimental process, the AuNPs remain in a dispersed state and the variations in absorbance and size of the AuNPs are minor. The novelty of this work lies in its adoption of CCT as the signal output, rather than using the absorbance or wavelength changes reported in most works as the signal output. By using a UV spectrometer to measure the kinetic curve of the absorbance of the sample solution at 400 nm over reaction time, CCT can be accurately determined, avoiding the cumbersome operation and errors caused by using absorbance and wavelength changes as signal outputs in the previous work. By employing the sensing strategy, Hg^{2+} can be analyzed ranging from 0 to 800 nM with a detection limit as low as 0.20 nM, which is much lower than the limit value (10 nM) set by the US Environmental Protection Agency (EPA) for drinking water.

Experimental section

Reagents and chemicals

Chloroauric acid ($HAuCl_4$), sodium citrate, and 4-nitrophenol were obtained from Sigma-Aldrich. Sodium borohydride ($NaBH_4$) was purchased from Alfa Aesar (Shanghai, China). The DNA sequence (5′-SH-TTTTTT TTTTTTTTTTTTTTTTTTTTTTTTT-3′) was synthesized by Sangon Biotechnology Co. Ltd. (Shanghai, China). The regents were of analytical grade and used without further purification. Ultrapure water (18.2 MΩ cm specific resistance) was used during the whole experiments. Twenty-millimolar Tris–HCl solution (pH 7.4) was employed as a buffer.

Instrumentation

UV–vis spectra were achieved by a Shimadzu UV-2550 spectrophotometer. The transmission electron microscope (TEM) was performed on a FEI F20. ICP-MS analyses were performed on PerkinElmer Elan DRC II (USA).

Synthesis of gold nanoparticles

AuNPs were synthesized according to the previous method [23]. Briefly, 250 mL of 1 mM aqueous $HAuCl_4$ solution was heated to 100 °C under vigorous stirring. Then, 25 mL of 38.8 mM sodium citrate was then added to the $HAuCl_4$ solution. Vigorous stirring of the above solution was continued for another 15 min at 100 °C. Finally, the solution was cooled to room temperature while being stirred continuously. The final AuNP solution was kept at 4 °C before use.

Measurement procedure of Hg^{2+}

Firstly, the processing of DNA is as follows: 1 μM of DNA in immobilized buffer (20 mM Tris–HCl containing 20 mM $MgCl_2$, 140 mM NaCl, and 1 mM TCEP, pH 7.40) was heated to 80 °C for 5 min and then cooled to room temperature. Then, 20 μL of 1 μM DNA was added to 200 μL of 1 nM AuNP solution for 12 h at 37 °C. After 12 h,
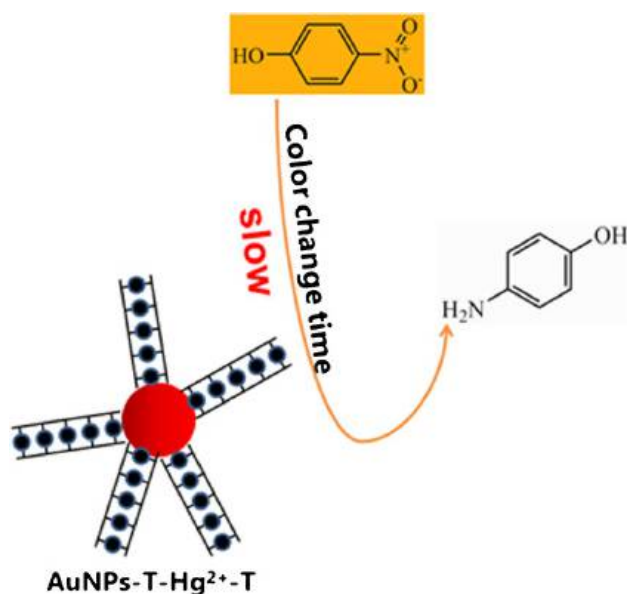
Scheme 1 Schematic illustration of the colorimetric method for detecting Hg^{2+} based on color change time as signal readout
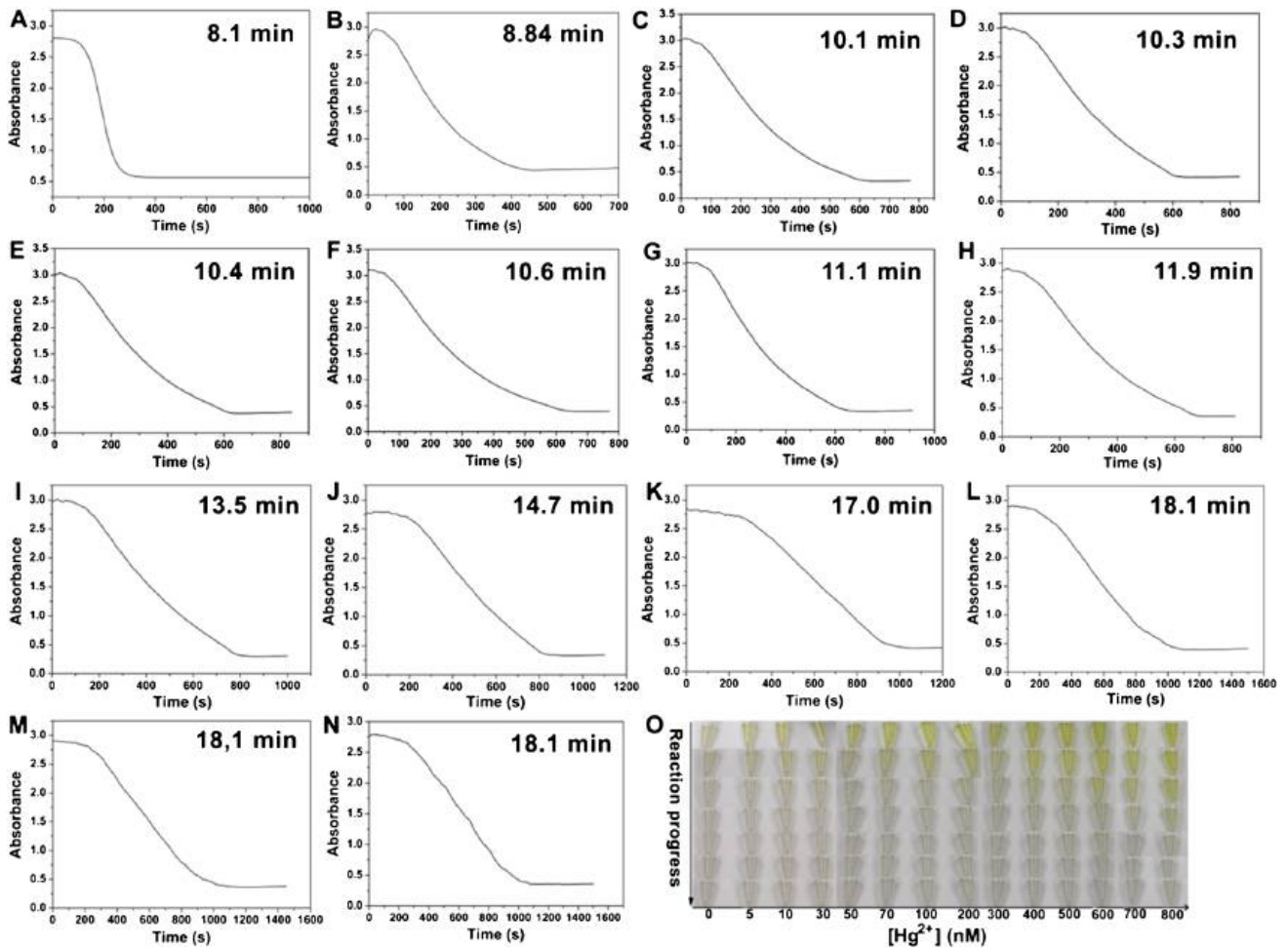
Fig. 1 Time-dependent curves of absorbance of the AuNP-DNA-p-nitrophenol-NaBH$_4$ solution containing different concentrations of Hg^{2+}: **A** 0 nM, **B** 5 nM, **C** 10 nM, **D** 30 nM, **E** 50 nM, **F** 70 nM, **G** 100 nM, **H** 200 nM, **I** 300 nM, **J** 400 nM, **K** 500 nM, **L** 600 nM, **M** 700 nM, and **N** 800 nM. **O** Progress in the reaction of p-nitrophenol and NaBH$_4$ catalyzed by AuNPs in the presence of different concentrations of Hg^{2+} ranging from 0 to 800 nM

Fig. 2 **A** CCTs of the solution as a function of Hg^{2+} concentrations. **B** The linear relationship between CCT and Hg^{2+} concentration in the range of 10–600 nM

$$CCT = 9.67 + 0.01[Hg^{2+}]$$
$$R = 0.99$$
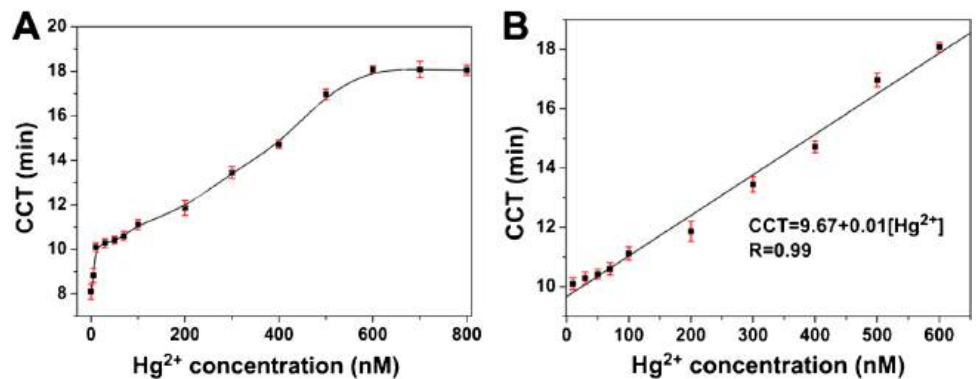
the solution was centrifuged at a speed of 1000 rpm for 5 min, and the DNA that was not connected to the AuNPs was poured out. Then, the DNA-functionalized AuNPs

below were redispersed in the same volume of AuNP solution. Next, different concentrations of Hg^{2+} solutions (5 μL) were added to the solution. Subsequently, 200 μL of

Table 1 Comparison of our work with other detection methods for Hg$^+$ detection

Methods	Materials	Linear range	LOD	Ref
C[a]	Aptamer-functionalized AuNPs	10–600 nM	0.20 nM	This work
C	p(PEGEMA)-b-p(DMAEMA)[d]-stabilized AuNPs	10 nM–3.5 μM	0.4 nM	[24]
C	KgM-AgNPs[e]	0.01–10 μM	3.25 nM	[25]
E[b]	Fe$_3$O$_4$@MPC/GCE[f]	1.0–4.0 μM	7.8 nM	[26]
F[c]	N,S-CDs[g]	20–100 nM	3.5 nM	[27]
E	GCE with polyL[h]	5 nM–3 μM	0.7 nM	[28]
F	SCDs[i]	0.05–5.8 μM	33.3 nM	[29]

[a]Colorimetric

[b]Electrochemical

[c]Fluorescent

[d]Poly(ethylene glycol methyl ether methacrylate)-b-poly(dimethylaminoethyl methacrylate)

[e]Hydrophilic konjac glucomannan-Ag nanoparticles

[f]Fe$_3$O$_4$@mesoporous carbon modified glassy carbon electrode

[g]N,S co-doped carbon dots

[h]glassy carbon electrode modified with poly(2,2′-(ethan-1,2-diylbis((2-(azulen-2-ylamino)-2-oxoethyl) azandiyl))diacetic acid

[i]Thioctic acid-carbon dots
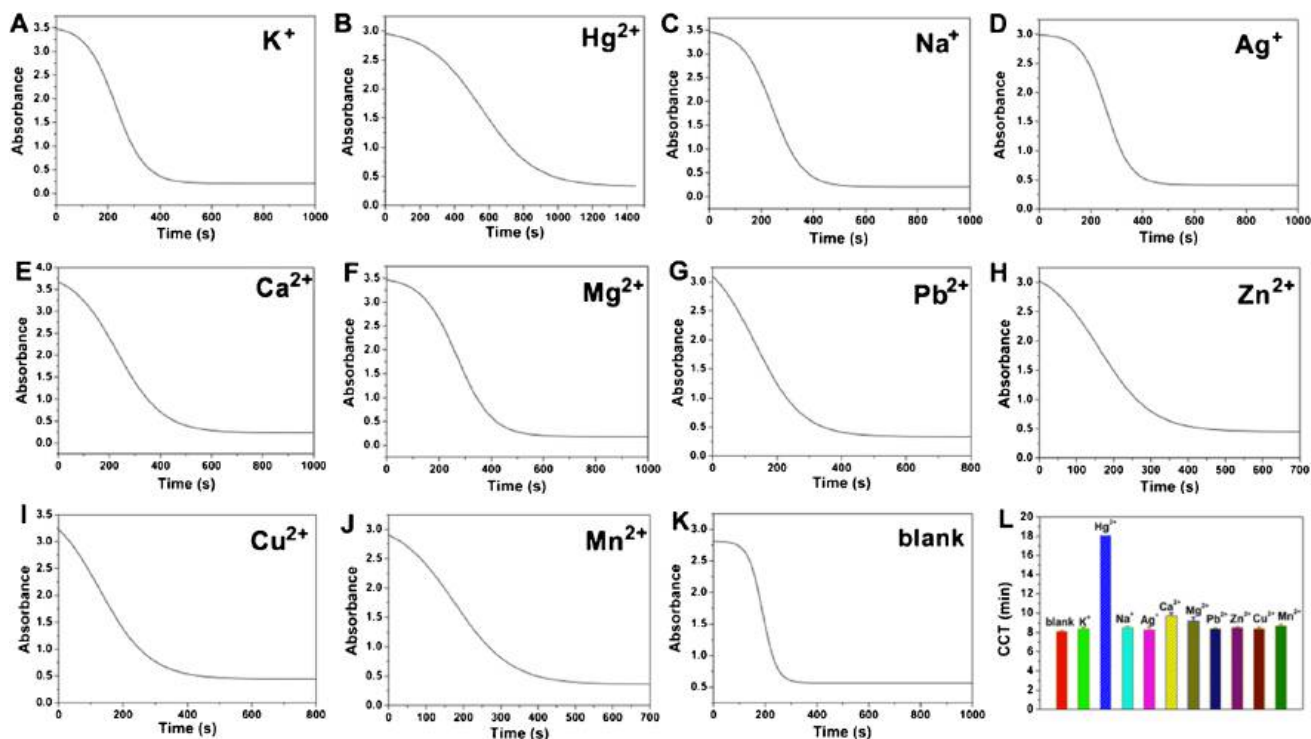
Fig. 3 Time-dependent curves of absorbance of the AuNP-DNA-p-nitrophenol-NaBH$_4$ solution in the presence of metal ions: **A** K$^+$, **B** Hg^{2+}, **C** Na$^+$, **D** Ag$^+$, **E** Ca^{2+}, **F** Mg^{2+}, **G** Pb^{2+}, **H** Zn^{2+}, **I** Cu^{2+}, **J** Mn^{2+}, and **K** blank 0.7 μM Hg^{2+}, 1 mM Ca^{2+}, 1 mM Mg^{2+}, and 70 μM other interfering metal ions. **L** CCT diagram of the solutions with different metal ions

freshly prepared NaBH$_4$ solution (0.24 M) and 50 μL of 1 mM p-nitrophenol was added into the mixture. The color of the solution is observed with the naked eye, and the color change time is measured through the kinetic curve of absorbance at 400 nm (which can be assigned to 4-nitrophenol) over time measured by a UV–vis spectrometer.
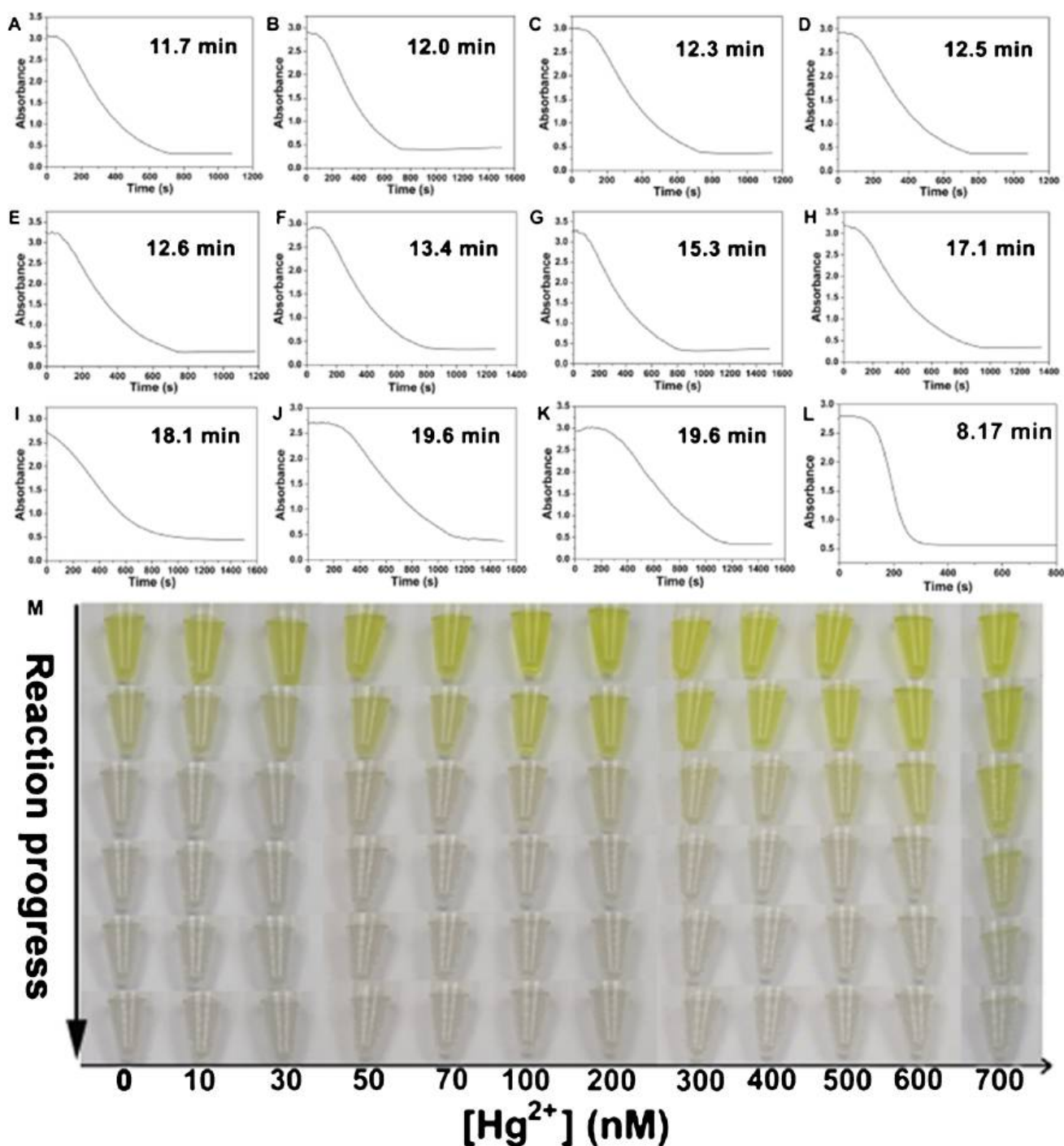
Fig. 4 Time-dependent curves of absorbance of the AuNP-DNA-p-nitrophenol-NaBH₄ solution containing different concentrations of Hg²⁺ in river water samples: **A** 10 nM, **B** 30 nM, **C** 50 nM, **D** 70 nM, **E** 100 nM, **F** 200 nM, **G** 300 nM, **H** 400 nM, **I** 500 nM, **J** 600 nM, **K** 700 nM, and **L** 0 nM. **M** Progress in the reaction of p-nitrophenol and NaBH₄ catalyzed by AuNPs in the presence of different concentrations of Hg²⁺ in river water ranging from 10 to 700 nM

Results and discussion

Factors affecting the colorimetric Hg²⁺ detection

For better sensing performance, the experimental conditions including DNA concentration, binding time of DNA and Hg²⁺, p-nitrophenol concentration, and NaBH₄ concentration were then optimized. We first explored the effect of DNA concentration on CCT. As shown in Figure S4, as the concentration of DNA increased, the CCT value of the reaction of p-nitrophenol and NaBH₄ catalyzed by AuNPs increased and gradually reached the maximum when DNA
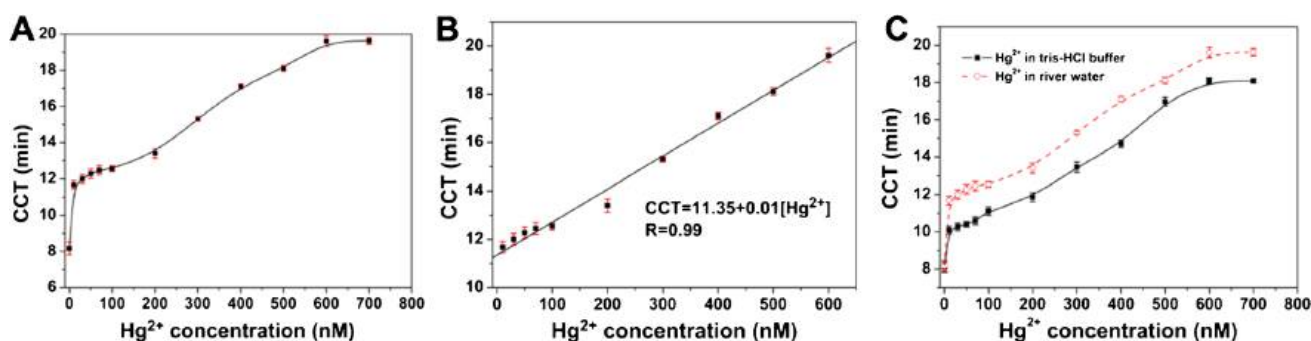
Fig. 5 A Plots of CCT versus different concentrations of Hg^{2+} (0–700 nM) in river water samples. **B** A linear relationship between CCT and Hg^{2+} concentration and the corresponding regression equation. **C** Comparison of CCT of mercury ions with different concentrations in river water and buffer

Table 2 Determination of Hg^{2+} in river water samples ($n=3$)

Sample	Hg^{2+} spiked (nM)	ICP-MS (nM)	This method (nM)	Recovery (%)
1	0	0	0	-
2	5.0	4.8 ± 0.05^a	5.1 ± 0.03	102
3	10.0	9.6 ± 0.08	9.8 ± 0.04	98

[a]Mean ± standard deviation of three determinations

concentration was 1 µM. Thus, 1 µM was chosen as the optimal concentration of DNA. Then, the binding time of DNA and Hg^{2+} was studied. As shown in Figure S5, the interaction of the DNA and Hg^{2+} is rather fast, which reached a balance within 10 min. So, 10 min was taken as the optimal incubation time of Hg^{2+}. The effect of p-nitrophenol concentration and $NaBH_4$ concentration was investigated (Figure S6 and Figure S7). As the concentration of p-nitrophenol increased, CCT gradually increased. $NaBH_4$ is the opposite. For economic and reaction time considerations, we have chosen 1 mM and 0.24 M as the optimal concentrations of p-nitrophenol and $NaBH_4$.

Sensitivity of the colorimetric assay for Hg^{2+}

Under the optimum conditions, the sensitivity of the assay for Hg^{2+} was evaluated. The CCTs of different concentrations of Hg^{2+} ranging from 0 to 800 nM are depicted in Fig. 1. As the reaction time progressed, the absorbance of each concentration of Hg^{2+} solution gradually decreased until reaching a plateau, indicating that the reaction between p-nitrophenol and $NaBH_4$ was complete. As Hg^{2+} concentrations ranged from 0 to 800 nM, the CCT value of the solutions increased gradually. Figure 2A shows the calibration curve of CCT versus the Hg^{2+} concentration; a linear relationship between CCT and Hg^{2+} concentration was acquired in the range of 10–600 nM. The regression equations were $CCT=9.67+0.01[Hg^{2+}]$ ($R=0.99$) (Fig. 2B). As we know, when it comes to the determination of

very low concentrations, the linear regression model will produce "y" values which are very close to the standard error. To avoid such situations, we drew a linear relationship for high concentrations of Hg^{2+} (Figure S8). The limit of detection (LOD) was calculated to be 0.20 nM according to the 3 σ/s rule. The LOD of Hg^{2+} is lower than the minimum mercury ion content (10 nM) in drinking water specified by the United States Environment Protection Agency. The sensitivity and linear range of the assay are better compared with some previously reported Hg^{2+} methods, as listed in Table 1. The high sensitivity of our Hg^{2+} assay arises from the CCT of the solution as the signal output, rather than traditional absorbance or wavelength changes as the signal output. The reproducibility of the assay was studied by performing 5 analyses on 100 nM Hg^{2+} solutions, with a relative standard deviation (RSD) of 2.9%.

Selectivity of the assay

Selectivity is another crucial factor in biosensors. To evaluate the selectivity of this assay for Hg^{2+}, we challenged the system with other interfering metal ions, including K^+, Na^+, Ag^+, Ca^{2+}, Mg^{2+}, Pb^{2+}, Zn^{2+}, Cu^{2+}, and Mn^{2+} (0.7 µM Hg^{2+}, 1 mM Ca^{2+}, 1 mM Mg^{2+}, and 70 µM other interfering metal ions). The assay was implemented under the same experimental procedures as Hg^{2+}. As shown in Fig. 3, when the reaction progressed to 9.7 min, all interfering ion solutions turned almost completely colorless yellow, while the color of 0.7 µM Hg^{2+} solution became colorless after 18 min of reaction. This indicates that DNA can selectively target Hg^{2+} due to the highly special affinity between T bases and Hg^{2+}. These results indicated that the DNA-functionalized AuNPs can function as a selective and anti-inference probe for Hg^{2+}.

Application in real samples

The method was used to measure Hg^{2+} in river water samples. The river water samples were first filtered through

a nylon film (0.45 μm) before extraction. Whether the river water needs to be diluted depends on the color of the water. If the river water itself appears yellow-green, then the sample needs to be diluted with secondary water to no color, so that the color of the diluted solution will not interfere with the color generated by the reaction of p-nitrophenol and sodium borohydride. Then, river water samples were spiked with Hg^{2+} in the concentration range of 10–700 nM and determined by the proposed method. Amazingly, by plotting color reaction progress (Fig. 4M) and kinetic curves of the absorbance change of Hg^{2+} with different concentrations over reaction time (Fig. 4A–L), similar to the detection of Hg^{2+} in standard solutions, the linear range of 10 to 600 nM was obtained with a regression coefficient of 0.99 (Fig. 5B). A linear relationship for high concentrations of Hg^{2+} in river samples is shown in Figure S9. Fortunately, the CCT curves caused by Hg^{2+} in the river water and buffer were almost parallel (Fig. 5C). Considering the impact of impurities in the river water, this result was still satisfactory. In addition, the river water samples were spiked with Hg^{2+} at varying concentrations (5 and 10 nM), respectively, and then analyzed using the proposed method and compared with the traditional inductively coupled plasma mass spectrometry (ICP-MS) as a reference standard. Table 2 shows a high degree of consistency between this method and ICP-MS in determining Hg^{2+} in river water samples. These results indicated the potentiality of the colorimetric method for Hg^{2+} detection in real water samples.

Conclusions

In this work, we presented a universal and effective colorimetric method for rapid and sensitive detection of Hg^{2+} in water samples. The biggest advantage of this method is that the kinetic curve of absorbance at 400 nm wavelength with reaction time can be used to determine the CCTs caused by Hg^{2+}. The colorimetric method was able to sensitively detect Hg^{2+} in buffer and river samples at the nM concentration level. No obvious interference of nine commonly interfering metal ions to Hg^{2+} detection was observed. The CCTs-based analytical method is expected to hold potentials in environmental monitoring and clinical diagnosis.

Declarations

Conflict of interest The authors declare no competing interests.

References

1. Srinivasan K, Subramanian K, Murugan K, Dinakaran K (2016) Sensitive fluorescence detection of mercury (II) in aqueous solution by the fluorescence quenching effect of MoS_2 with DNA functionalized carbon dots. Analyst 141:6344–6352
2. Ajsuvakova OP, Tinkov AA, Aschner M, Rocha JBT, Michalke B, Skalnaya MG, Skalny AV, Butnariu M, Dadar M, Sarac I, Aaseth J, Bjorklund G (2020) Sulfhydryl groups as targets of mercury toxicity. Coord Chem Rev 417:213343
3. Liu JW, Lu Y (2007) Rational design of "turn-on" allosteric DNA-zyme catalytic beacons for aqueous mercury ions with ultrahigh sensitivity and selectivity. Angew Chem Int Ed 46:7587–7590
4. Li LB, Zhang JY, Zhao WL, Liu XH, Luo LJ, Bi XY, Cheng L, You TY (2021) DNA-modified electrochemiluminescent tris(4,4′-dicarboxylicacid-2,2′-bipyridyl) ruthenium(II) dichloride and assistant DNA-modified carbon nitride quantum dots for Hg^{2+} detection. ACS Appl Nano Mater 4:1009–1018
5. Chen GH, Chen WY, Yen YC, Wang CW, Chang HT, Chen CF (2014) Detection of mercury(II) ions using colorimetric gold nanoparticles on paper-based analytical devices. Anal Chem 86:6843–6849
6. Karami C, Taher MA, Shahlaei M (2020) A simple method for determination of mercury(II) ions by PNBS-doped carbon dots as a fluorescent probe. J Mater Sci Mater Electron 31:5975–5983
7. Ncube P, Krause RWM, Ndinteh DT, Mamba BB (2014) Fluorescent sensing and determination of mercury (II) ions in water. Water SA 40:175–182
8. Gao Y, Liu M, Yue X, Du J (2019) Ratiometric fluorometric determination of mercury (II) by exploiting its quenching effect on glutathione-stabilized and tetraphenylporphyrin modified gold nanoclusters. Microchim Acta 186:307
9. Manzoor A, Kokab T, Nawab A, Shah A, Siddiqi HM, Iqbal A (2022) Electrochemical detection of mercuric(ii) ions in aqueous media using glassy carbon electrode modified with synthesized tribenzamides and silver nanoparticles. RSC Adv 12:1682–1693
10. Matlou GG, Nkosi D, Pillay K, Arotiba O (2016) Electrochemical detection of Hg (II) in water using self-assembled single walled carbon nanotube-poly(m-Amino benzene sulfonic acid) on gold electrode. Sens Biosensing Res 10:27–33
11. Liu SJ, Nie HG, Jiang JH, Shen GL, Yu RQ (2009) Electrochemical sensor for mercury (II) based on conformational switch mediated by interstrand cooperative coordination. Anal Chem 81:5724–5730
12. Lee JS, Han MS, Mirkin CA (2007) Colorimetric detection of mercuric ion (Hg^{2+}) in aqueous media using DNA-functionalized gold nanoparticles. Angew Chem Int Ed 46:4093–4096
13. Logan N, McVey C, Elliott C, Cao C (2020) Amalgamated gold-nanoalloys with enhanced catalytic activity for the detection of mercury ions (Hg^{2+}) in seawater samples. Nano Res 13:989–998
14. Long YJ, Li YF, Liu Y, Zheng JJ, Tang J, Huang CZ (2011) Visual observation of the mercury-stimulated peroxidase mimetic activity of gold nanoparticles. Chem Commun 47:11939–11941
15. Wu LL, Wang LY, Xie ZJ, Xue F, Peng CF (2016) Colorimetric detection of Hg2+ based on inhibiting the peroxidase-like activity of DNA-Ag/Pt nanoclusters. RSC Adv 6:75384–75389

16. Jiang Y, Zhao H, Lin Y, Zhu N, Ma Y, Mao L (2010) Colorimetric detection of glucose in rat brain using gold nanoparticles. Angew Chem Int Ed 49:4800–4804

17. Guo Y, Wang Z, Shao H, Jiang X (2012) Stable fluorescent gold nanoparticles for detection of Cu^{2+} with good sensitivity and selectivity. Analyst 137:301–304

18. Bhai S, Ganguly B (2020) Role of the backbone of nucleic acids in the stability of Hg^{2+}-mediated canonical base pairs and thymine-thymine mispair: a DFT study. RSC Adv 10:40969–40982

19. Zhang Z, Tang A, Liao S, Chen P, Wu Z, Shen G, Yu R (2011) Oligonucleotide probes applied for sensitive enzyme-amplified electrochemical assay of Mercury(II) ions. Biosens Bioelectron 26:3320–3324

20. Keshavarzi P, Abbasi-Moayed S, Khodabakhsh M, Unal U, Hormozi-Nezhad MR (2023) Chrono-colorimetric sensor array for detection and discrimination of halide ions using an all-in-one plasmonic sensor element. Talanta 259:124528

21. Zhang M, Liu YQ, Ye BC (2011) Colorimetric assay for sulfate using positively-charged gold nanoparticles and its application for real-time monitoring of redox process. Analyst 136:4558–4562

22. Kostara A, Tsogas GZ, Vlessidis AG, Giokas DL (2018) Generic assay of sulfur-containing compounds based on kinetics inhibition of gold nanoparticle photochemical growth. ACS Omega 3:16831–16838

23. Turkevich J, Stevenson PC, Hillier J (1951) A study of the nucleation and growth processes in the synthesis of colloidal gold. Discuss Faraday Soc 11:55–75

24. Preman NK, Jain S, Antony A, Shetty DM, Fathima N, Prasad KS, Johnson RP (2023) Stimuli-responsive copolymer-mediated synthesis of gold nanoparticles for nanozyme-based colorimetric detection of mercury(II) ions. ACS Appl Polym Mater 5:6377–6389

25. Jayeoye TJ, Eze FN, Olatunji OJ, Tyopine AA (2022) Synthesis of biocompatible konjac glucomannan stabilized silver nanoparticles, with asystasia gangetica phenolic extract for colorimetric detection of mercury (II) ion. Sci Rep 12:9176

26. Liu YZ, Wu SY, Xiong W, Li H (2023) Interface Co-assembly synthesis of magnetic Fe_3O_4@mesoporous carbon for efficient electrochemical detection of Hg(II) and Pb(II). Adv Mater Interfaces 10:2201631

27. Khan WU, Qin LY, Chen LX, Khan WU, Zeb S, Khan A, Li SZ, Khan SU, Kamal S, Zhou P (2023) High biocompatible nitrogen and sulfur Co-doped carbon dots for Hg(II) detection and their long-term biological stability in living cells. Anal Chim Acta 1245:340847

28. Pirvu C, Stanciu G, Buica GO (2022) Cu(II) and Hg(II) detection under photo-assisted accumulation in an open circuit potential at a polyazulene-EDTA like modified electrode. Analyst 147:4730–4734

29. Wang S, Chen HY, Xie HL, Wei LN, Xu L, Zhang L, Lan W, Zhou CS, She YB, Fu HY (2021) A novel thioctic acid-carbon dots fluorescence sensor for the detection of Hg^{2+} and thiophanate methyl via S-Hg affinity. Food Chem 346:128923